MASS FLOW MEASUREMENT OF GRANULAR MATERIALS IN AERIAL APPLICATION — PART 2: EXPERIMENTAL MODEL VALIDATION

T. E. Grift, J. T. Walker, J. W. Hofstee

ABSTRACT. *A system was developed to measure the mass flow of granular fertilizer material in aerial spreader ducts. The flow process was regarded as the sequential passage of clusters containing multiple particles with varying diameters. An optical sensor was used to measure the cluster lengths on the fly. In a low–density flow regime, the diameter of each particle could be measured individually (this is called the "single–particle approach"). After conversion to a volume of a sphere and multiplication by the true material density, the mass flow could be computed. In a high–density mass flow regime (called the "mass flow approach"), particles form clusters, and cluster lengths would be measured instead of particle diameters. The first step in performing mass flow measurement was to develop a reconstruction algorithm that estimates the number of particles in a cluster from the measured cluster length. This algorithm, called the Exponential Estimator, was developed using simulation and is reported in Part 1. This article, Part 2, describes the use of the mass flow sensor as well as the reconstruction algorithm to assess the accuracy of the complete system. Tests were carried out under laboratory conditions, using mass flows of spherical particles as well as urea fertilizer under varying flow velocities and densities. The mass flow of identical spherical particles of 4.45 mm diameter was measured with an accuracy of 3%, even under high–density flow conditions. For granular fertilizer, the flow was measured with an accuracy of 2% for high–density flows and 4% for low–density flows.*

Keywords. *Mass flow measurement, Clustering process, Aerial application, Fertilizer, MatLab™.*

Agricultural aircraft are widely used in the United States and many other countries for applying granular fertilizers and pesticides. Aerial application of granular materials involves metering the material into the spreader at a desired application rate and uniformly distributing it over the target area. The required material flow rate is governed by several factors, including swath width and aircraft speed. The ideal swath width and uniformity of distribution further depend upon such factors as spreader design, physical characteristics of the applied material, release height, and wind velocity. Although the application equipment is usually calibrated once per year (Gardisser and Walker, 1990), aerial application frequently results in uneven distribution of applied materials, causing yield loss (Grift et al., 2000; Helms et al., 1987). Other potential problems are over–dosing and non–target application on the ends and sides of the treated area. This poses environmental risk and the potential for damage to crops in neighboring fields.

For spraying applications, controller systems that integrate GPS information with the output rate are used to ensure a constant rate on the ground. For granular material application, no such device is available. Often pilots rely on experience to adjust the spreader output in cases of head or tail wind. Without a direct feedback mechanism, this method is unreliable.

An accurate flow sensor for granular material output of the entire spreader would give the pilot much more control over his work. Furthermore, if a sensor were placed in each spreader duct, landing positions on the ground of the material from each duct could be predicted. This system would effectively monitor the lateral distribution of fertilizer. When integrated with a GPS flight guidance system and controlled gate/vane geometry, the system would produce uniform spread patterns automatically.

The flow sensor developed in this study could be the key component to a modern, precision agriculture approach to aerial application of granular materials in the near future.

The objectives of this study were:

- To develop and test a system that measures the mass flow of granular fertilizer particles in an aerial spreader duct.
- To determine the limits of the system accuracy, in relation to flow velocity and density.

Article was submitted for review in January 2000; approved for publication by the Power & Machinery Division of ASAE in October 2000.

The authors are **Tony E. Grift,** ***ASAE Member Engineer,*** Assistant Professor, Department of Biosystems Engineering, Auburn University, Auburn, Alabama; **Joel. T. Walker,** ***ASAE Member Engineer,*** Professor, Department of Biological and Agricultural Engineering, University of Arkansas, Fayetteville, Arkansas; and **Jan Willem Hofstee**, ***ASAE Member Engineer,*** Associate Professor, Department of Agricultural, Environmental, and Systems Technology, Wageningen University and Research Center, Wageningen, The Netherlands. **Corresponding author:** Tony E. Grift, 213 Tom E. Corley Bldg, Auburn University, Auburn, AL 36849; phone: 334–844–3545; fax: 334–844–3530; e–mail: tegrift@eng.auburn.edu.

MATERIALS AND METHODS

OPTICAL SENSOR

Grift and Hofstee (1997) developed an optical sensor that measures the length of clusters of fertilizer particles on the fly. This optical mass flow sensor is shown in figure 1. It consists of a light source and two infrared photo sensor arrays that act as digital on/off switches. The array output is normally "high." It becomes "low" when the light projected onto the array is blocked. The lenses magnify the image of the clusters to improve the accuracy.

© 2001 American Society of Agricultural Engineers

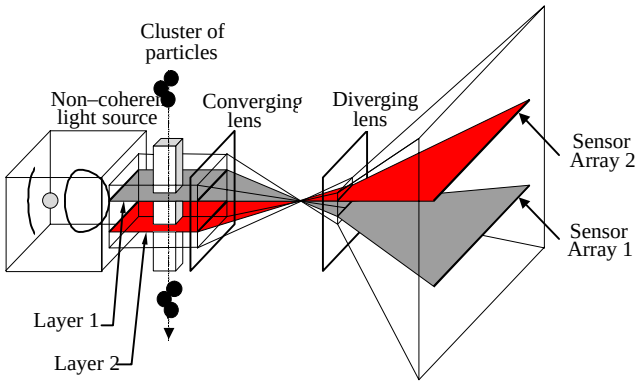

Figure 1. Principle of optical mass flow sensor.

The velocity and length of a cluster can be determined using the output signals of the two sensor arrays during the passage of a cluster. This principle is shown in figure 2, where four events are frozen in time. When a cluster blocks layer 1 (event 1), the output of array 1 becomes "low." When the cluster unblocks the layer (event 3), the output becomes "high." The process is similar for layer 2/array 2 (events 2 and 4).

The velocity of a cluster is the distance between the sensor arrays divided by the time between blocking events of layer 1 and layer 2:

$$v = \frac{b}{\Delta t_f} \tag{1}$$

where

v = velocity of the cluster (ms^{-1})
b = distance between the sensor arrays (0.885 mm)
Δt_f = time between blocking events of layer 1 (event 1) and layer 2 (event 2)

The total time a cluster blocks either layer (from event 1 to 3, or from event 2 to 4) is Δt_p. The cluster length can now be computed by multiplying the total layer blocking time (Δt_p) by the cluster velocity:

$$D = v\Delta t_p = b\frac{\Delta t_p}{\Delta t_f} \tag{2}$$

where D is the length of the cluster (m). Note that the cluster length measurement is independent of the velocity value. For example, if the velocity doubles, then Δt_f will halve, and so will Δt_p. Hence, the ratio remains constant.

The following assumptions were made with regard to cluster length measurement: 1) the cluster velocity remains constant during detection, and 2) no cluster reorganization occurs during the cluster passage. Both assumptions are reasonable because the distance between layer 1 and layer 2 is very small (0.885 mm), and hence the detection time is very short (typically in the millisecond range).

The timing signals (Δt_f and Δt_p) and the total experiment time were measured using a TC 1024 Timer Board (Real Time Devices USA, Inc., State College, Penn.) under control of an interrupt–based program written in C.

The most important source of error in the optical sensor is defocus, which occurs when particles pass the sensor away from the optical focal plane. This error is unavoidable. It is caused by the non–coherent light source used in the design. This light source has the advantage of not requiring precise alignment of the sensor arrays as, for example, a laser light source would. This is very important when the sensor is to be applied in harsh environments such as an airplane in flight.

Sensor Calibration

To assess the magnitude of errors during cluster length measurement, fifty identical spherical steel balls were dropped through the sensor by hand from a height of 5 cm. The diameter of the steel balls was 4.45 mm, as measured with a slide micrometer. The balls achieved a velocity of about 1 ms^{-1} at the moment they were detected. After dropping the fifty steel balls, the distance between the light–sensitive layers (b in fig. 2) was adjusted to 0.885 mm to yield a mean particle diameter of 4.45 mm. The histogram of the measured diameters is shown in figure 3. The shape suggests that the distribution is normal, and a normality test in the statistical analysis program JMP (Sall and Lehman, 1996) confirmed this with 96% probability. The mean was 4.45 mm (calibrated) and the standard deviation was 0.15 mm. These values were used in the "thresholding" process, which will be described later.

Exponential Estimator As Reconstruction Algorithm

The basic approach to mass flow measurement in this study was determination of the number of passing particles in a flow during a specific time period. In the "mass flow approach" (MFA), the lengths of clusters are measured, rather than the diameters of individual particles. Therefore, a method that reconstructs the original number of particles from measured cluster lengths must be applied. This reconstruction algorithm, called the "Exponential Estimator," was developed by simulating clustering processes in MatLab (1997), as explained in Part 1 (Grift, 2001). The results of this research are briefly mentioned here.

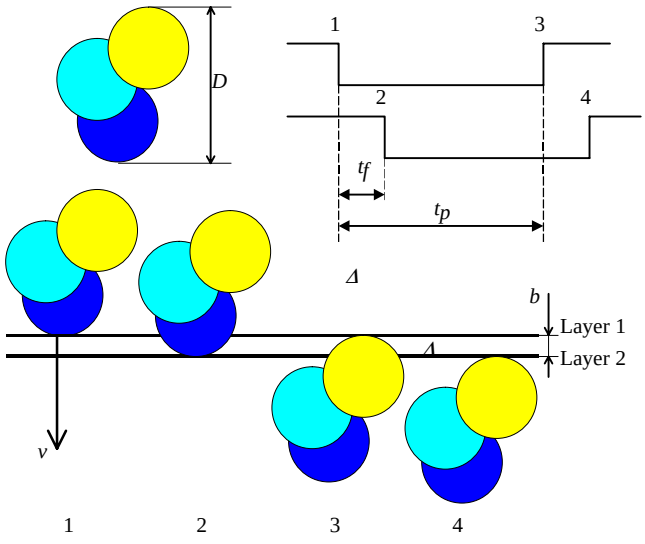

Figure 2. Cluster length measurement with mass flow sensor.

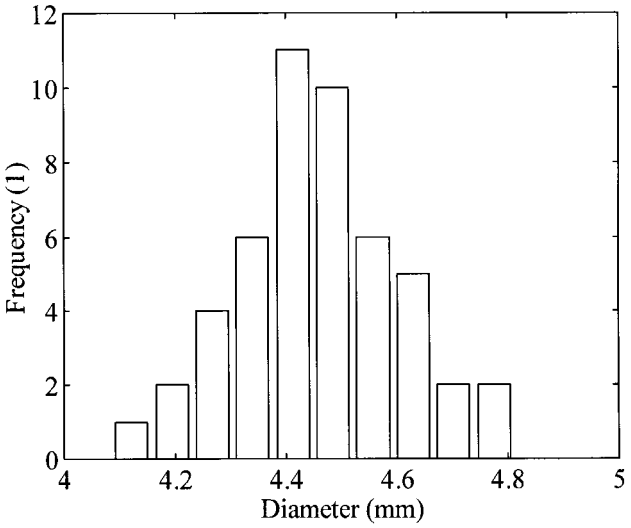

Figure 3. Measured diameter distribution of 4.45 mm particles determined by dropping 50 identical steel balls individually through the optical sensor.

Event Ratio (ER)

This dimensionless variable is the ratio of the total number of particles used in an experiment and the total number of measured clusters that resulted. When the density of the flow is extremely low, each particle is measured separately, and the event ratio becomes "1." This case, in which no clustering occurs, is termed the "single–particle approach" (SPA) and, as mentioned, can only exist for very sparse flow regimes. In formula form:

$$ER = \frac{E}{N} \tag{3}$$

where

E = number of cluster detections (events)
N = number of particles per experiment

The event ratio is known in a laboratory experiment, which is performed with a known number of initial particles (N). In a practical situation, N is the quantity that must be determined to perform the mass flow measurement. The number of clusters (E) in a specific time frame can be measured directly in a lab experiment as well as in practice.

Occupancy Rate (OR)

This dimensionless variable is the measure of the flow density. It was chosen on intuition and based on the total amount of space that is occupied by the particles (the "particle–space") divided by the total length of "space" that passes during a specific time period. In an experiment, the total amount of particle–space is simply the total length of all individual particles used. The total length of "space" that passes is equal to the mean velocity of the clusters, which is measured, multiplied by the total duration of the experiment. In formula form:

$$OR = \frac{N\overline{D}}{\overline{v}t} \tag{4}$$

where

N = total number of particles
$\overline{D}$ = mean diameter of the particles (m)
$\overline{v}$ = mean velocity of the particles (ms^{-1})
t = total duration of the experiment (s)

In a laboratory experiment, all components of the occupancy rate are available. The total number of particles (N) and the mean diameter of the particles ($\overline{D}$) are already known, and the total duration of the experiment (t) and the mean cluster velocity ($\overline{v}$) are measured. In practice, there is a continuous flow, and N and $\overline{D}$ would not be known or measurable in a chosen time frame. However, simulations showed that the occupancy rate can be measured indirectly through two measurable quantities, as described later.

Cluster Order

In the case of identical particles with diameters D, "singles" were defined as clusters with length D (they are in fact single particles), "doubles" were defined as clusters with lengths in the range [D,2D], "triples" as clusters with lengths in the range [2D,3D], and so on. Note that the name "triple" does not imply that the cluster is composed of three particles. Depending upon the cluster configuration, four or even five particles can form a cluster with a length in the [2D,3D] range and be termed a triple. A cluster that contains n particles was termed an "n–particle cluster."

In practice, measured particle diameters are always distributed. Even the measured diameters of identical particles contain small errors. For distributed particle diameters with mean diameter μ and standard deviation σ, the categorization process was defined as follows: singles are clusters with lengths in the range [0, μ+3σ], doubles are clusters with lengths in the range [μ+3σ,2μ+3σ], and triples are clusters with lengths in the range [2μ+3σ,3μ+3σ].

This categorization process is termed "thresholding" and can be performed in real time. Singles, doubles, triples, etc., are referred to as clusters of order 1, 2, 3, etc., respectively. The total number of clusters per order is therefore indicated by the symbols N_0 for singles, N_1 for doubles, N_2 for triples, and so forth.

Relationships

Simulations revealed a very simple relationship between the event ratio (ER) and the occupancy rate (OR):

$$ER = \frac{E}{N} = e^{-\alpha_1 OR} \tag{5}$$

The value of α_1 was found to be unity for all four particle–diameter cases tested in simulation: identical, uniformly distributed, normally distributed, and urea–distributed. Because the number of events per time period is known, the total number of particles in the experiment (N) can be estimated by rewriting equation 5:

$$N_{EST} = E\, e^{\alpha_1 OR} \tag{6}$$

where N_{EST} = estimated number of particles.

Another simple relationship was discovered between the measurable ratio of doubles–singles and the occupancy rate (OR):

$$OR = \alpha_2 \frac{N_1}{N_0} \quad (7)$$

In simulation, the value of α_2 was found to be unity for identical–diameter particles. In the distributed–diameter cases, the relationship was still linear, but the slope was no longer unity. The complete reconstruction formula based on the ratio of doubles–singles is now:

$$N_{EST1\_0} = E\, e^{\alpha_1 \alpha_2 (N_1/N_0)} \quad (8)$$

or with $\alpha_3 = \alpha_1 \alpha_2$:

$$N_{EST1\_0} = E\, e^{\alpha_3 (N_1/N_0)} \quad (9)$$

where

N_{EST1_0} = Exponential Estimator based on the ratio of doubles–singles
E = number of cluster detections (events)
α_3 = constant (depends on the particle diameter distribution)
N_1 = number of doubles
N_0 = number of singles

Experimental Validation of Exponential Estimator

The complete Exponential Estimator formula (eq. 9) was validated by dropping 2000 particles from four different heights (30, 46, 54, and 101 cm) to obtain different flow densities. The particles were fed through a PVC pipe with an internal diameter of 2.54 cm by dropping all particles at once into a funnel that was placed on top of the pipe. The separation of particles due to gravitational acceleration resulted in varying flow densities or occupancy rates. The experimental validation of the Exponential Estimator model was performed using a four–step approach:

1. Validation of equation 5:

$$ER = e^{-\alpha_1 OR}$$

For each experiment, the occupancy rate (*OR* in eq. 4) was computed from the total length of all particles per experiment (number of particles times the mean particle diameter determined off–line) and divided by the total "space" that passed the sensor during the experiment (mean cluster velocity times total experiment time).

The event ratio (*ER* in eq. 3) was computed from the number of detected clusters per experiment (*E*) divided by the number of particles in the experiment (*N*). The number of doubles and singles per experiment was determined by thresholding.

The validity of equation 5 was determined by plotting *OR* against the natural logarithm of *ER* and fitting a straight line through the data in an Ordinary Least Squares sense with the origin as a fixed point. This approach can be justified as follows: When the event ratio is "1" (and its logarithm is "0"), then the number of events (*E*) is equal to the number of particles (*N*), and hence, all particles are measured individually. This can only be the case when the flow is extremely sparse and the occupancy rate tends to "0." The slope of the regression line was used to determine that α_1 = –(1/*slope*).

2. Validation of equation 7:

$$OR = \alpha_2 (N_1/N_0)$$

The parameter α_2 was determined for identical–diameter particles (4.45 mm) as well as urea–fertilizer particles. Although in simulation the value of α_2 for identical particles was "1," in practice the measurements have small variations due to measurement errors, causing α_2 to differ from unity.

Equation 7 was validated by simply plotting the ratio of doubles–singles against the occupancy rate and, as with equation 5, fitting a straight line through the data in an Ordinary Least Squares sense. The origin was used as a fixed point because the occupancy rate tending to "0" implies the single–particle approach, in which no particle overlap occurs and the number of doubles (N_1) is "0." The slope of the regression line was used to determine that α_2 = (1/*slope*).

3. Validation of the combination of equations 5 and 7:

$$ER = e^{-\alpha_3 (N_1/N_0)}$$

Here, the relationship was converted to:

$$\ln ER = -\alpha_3 \frac{N_1}{N_0} \quad (10)$$

and the ratio of doubles–singles was plotted against the natural logarithm of the event ratio. As before, a straight–line regression was performed with the origin as a fixed point, and α_3 = –(1/*slope*).

4. Validation of equation 9:

$$N_{EST1\_0} = E\, e^{\alpha_3 (N_1/N_0)}$$

The complete Exponential Estimator was validated by plotting the ratio of the estimated number of particles per experiment and the true number of particles (N_{EST1_0}/N) against the occupancy rate. This resulted in a normalized accuracy plot, with which the variability of the accuracy for higher occupancy rates can be studied.

Results and Discussion

All experiments were carried out with 2000 initial particles. In figures 4 and 7, the data is organized as follows: The top–left subplot (a) shows the sorted measured cluster lengths for an arbitrarily chosen occupancy rate (0.91 for identical particles, 0.42 for urea particles). The other subplots represent the validation of the three relationships described in the preceding section: equation 5 (subplot b), equation 7 (subplot c), and the combination of equations 5 and 7 (subplot d). Figures 5 and 8 represent the normalized accuracy plots for identical and urea particles, respectively.

Experiments With Identical–Diameter Particles (4.45 mm)

Fifty experiments were conducted with identical spherical steel balls of 4.45 mm diameter. In figure 4a, the sorted cluster lengths are shown from a single 2000–particle experiment for a high–density flow (*OR* = 0.91). The shape of the plot indicates a significant number of singles

([0, ≈300]), a linear increase for doubles ([≈300, ≈600]), and a seemingly non–linear increase for higher–order clusters.

The horizontal solid lines are the transitions between cluster orders determined by thresholding. The measured mean of the identical particles was 4.45 mm and the standard deviation was 0.15 mm. The single–double transition is therefore: 4.45 + (3 × 0.15) = 4.9 mm.

The first validation step was observing the relationship $ER = e^{-\alpha_1 OR}$ (eq. 5). Simulations had shown that this relationship was independent of the diameter distribution of the particles. In figure 4b, the occupancy rate is plotted against the natural logarithm of the event ratio. The slope of the no–intercept regression line is –0.99, yielding $\alpha_1 = 1.01$, which is indeed very close to the simulation value of "1."

The second validation step was observing the relationship $OR = \alpha_2 (N_1/N_0)$ (eq. 7). This relationship is shown in figure 4c. Again, a straight–line behavior was found, and the slope of the no–intercept regression line is 1.04, or $\alpha_2 = 0.96$, also close to the simulation value of "1."

The third validation step was the product of the two previous steps, and represents the complete Exponential Estimator: $ER = e^{-\alpha_3 (N_1/N_0)}$. Figure 4d plots the ratio of doubles–singles against the natural logarithm of the event ratio. A no–intercept straight line was fitted in an Ordinary Least Squares sense, leading to a slope of –1.03, or $\alpha_3 = 0.97$.

Figure 5 shows the normalized accuracy (N_{EST1_0}/N), in which the total reconstructed number of particles was divided by 2000 (that is, by the actual number of particles). The (trivial) mean accuracy of the measurements was 1.00 (calibrated with $\alpha_3 = 0.97$) and the standard deviation was 0.03. The accuracy becomes significantly more variable for occupancy rates higher than 0.5. This error could be reduced by measuring with more particles (longer time period).

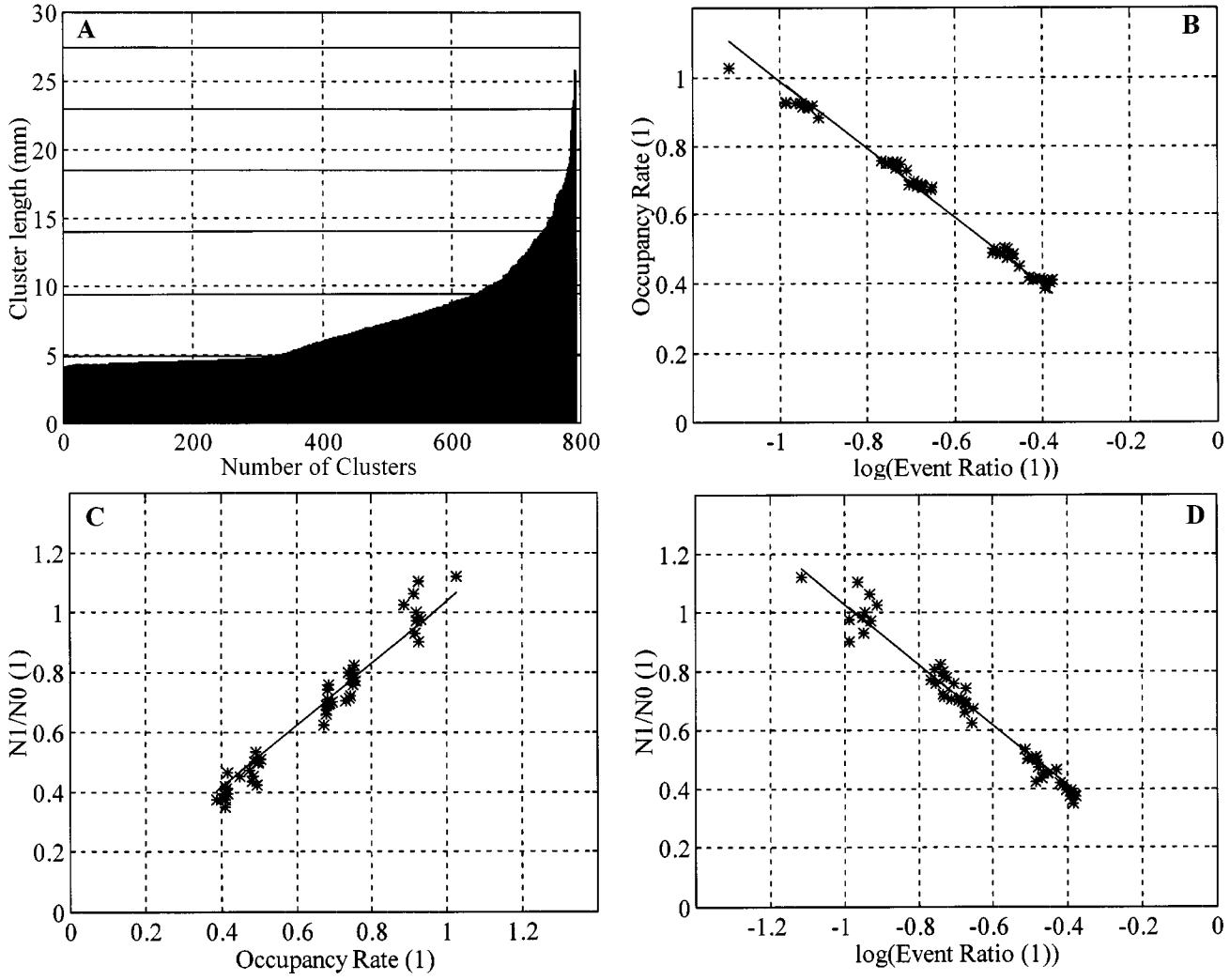

Figure 4. Measured sorted cluster lengths (*OR* = 0.91, 2000 initial particles) and functional relationships for identical–diameter particles (4.5 mm).

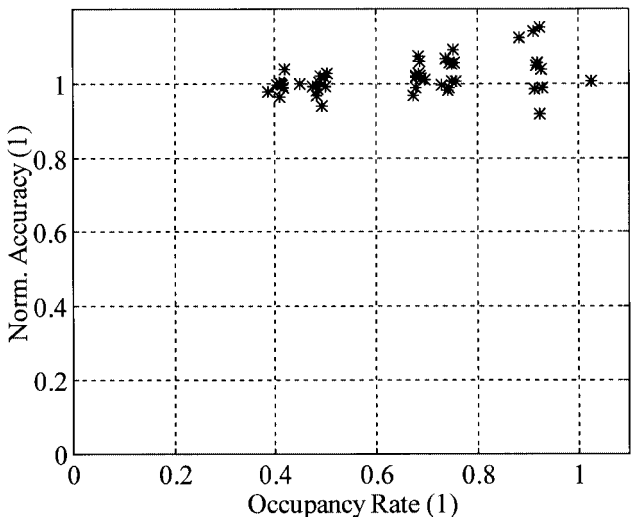

Figure 5. Normalized accuracy (1) of Exponential Estimator from 50 identical particle experiments (2000 particles each).

Experiments with Urea Fertilizer

As in the identical–diameter case, the thresholding process (determination of the transitions between the measured cluster orders) requires measurement of the size distribution of the particles. Figure 6 shows the diameter distribution of urea fertilizer particles, as observed by the mass flow sensor. This distribution was determined from a test in which 600 randomly selected urea particles were dropped individually through the sensor from a height of 5 cm. At the moment of detection, they reached a velocity of about 1 ms^{-1}. The mean of the distribution is 2.58 mm, and the standard deviation is 0.41 mm. As the plot suggests, the distribution is not normal. This was confirmed by a normality test using the statistical analysis program JMP (Sall and Lehman, 1996).

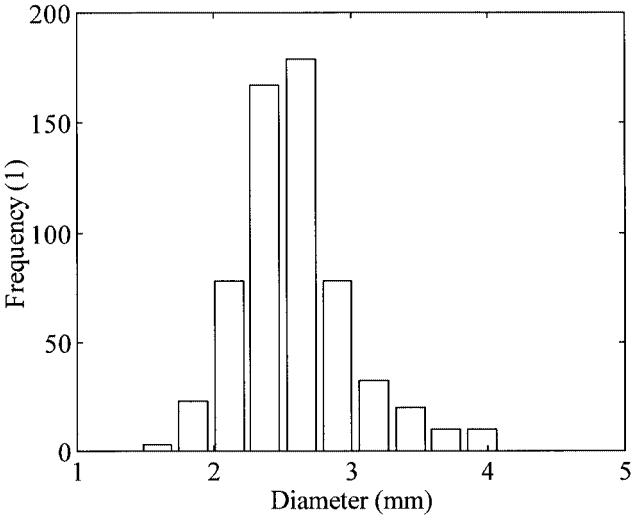

Figure 6. Measured diameter distribution of urea fertilizer determined by dropping 600 particles individually through the optical sensor.

High–Density Urea Experiments

Ten experiments with urea fertilizer were conducted at higher densities, with occupancy rates in the range [0.25,0.42]. The sorted cluster lengths of a single experiment (OR = 0.42) are shown in figure 7a. As in figure 4a, the horizontal solid lines represent the transitions between cluster orders. For example, according to the definition of "thresholding" for distributed–diameter particles, the transition between singles and doubles is 2.58 + (3 × 0.41) = 3.81 mm. Figure 7b plots the occupancy rate against the natural logarithm of the event ratio. The straight–line regression yielded a slope of –0.84, or α_1 = 1.19. Simulation showed that this value should be "1," independent of the distribution of the particle diameters. Figure 7c plots the ratio of double–singles against the occupancy rate. The straight–line regression resulted in a value for α_2 of 0.57. The parameter α_3 was determined from a straight–line regression, as shown in figure 7d, again with the origin as a fixed point. It yielded a slope of –0.48, leading to α_3 = 2.07.

In figure 8, the normalized accuracy of the Exponential Estimator (N_{EST1_0}/N) is plotted against the occupancy rate. The (trivial) mean accuracy was 1.00 (calibrated with α_3 = 2.07) and the standard deviation was 0.02, for a maximum occupancy rate of 0.42.

Low–Density Urea Experiments

In aerial spreaders, the smallest fertilizer particles can reach velocities up to 27 ms^{-1}, depending on their location within the spreader (Bansal, 1997). To test the sensor's detection–speed limitations, experiments were carried out by dropping particles into the fall pipe from a height of 1.40 m under air suction, which created a low–density, high–velocity flow. The mean velocity among 25 experiments was 14.6 ms^{-1}. At this velocity, approximately 550 clusters per second were detected, which shows that the sensor hardware is very well suited to measure high–velocity mass flows. The accuracy of the Exponential Estimator for low–density flows was 1.00 (calibrated with α_3 = 2.07, as determined in the high–density urea experiments) and the standard deviation was 0.04. The accuracy of the sensor may be expected to be high under low–density conditions because most of the particles are measured individually rather than as clusters.

Comparison of Simulation and Experiment Results

In table 1, the parameters (α_1, α_2, and α_3) of the Exponential Estimator are summarized for identical–diameter particles and urea fertilizer particles in simulation and in experiment. For identical–diameter particles, the reconstruction algorithm proved to be quite accurate. In simulation, the values for both α_1 and α_2 were found to be "1," and the measured values are close (1.01 and 0.96, respectively).

For urea fertilizer, the differences were found to be much greater. In simulation, α_1 was found to be "1" (independent of the diameter distribution), but it was measured as 1.19. Parameter α_2 was found to be 1.8 in simulation, and it was measured as 1.74. The most important parameter, α_3, had a value of 1.8 in simulation and was measured as 2.07. Whether these differences must be attributed to the measurement system, the simulation procedure, or the thresholding method is presently unclear.

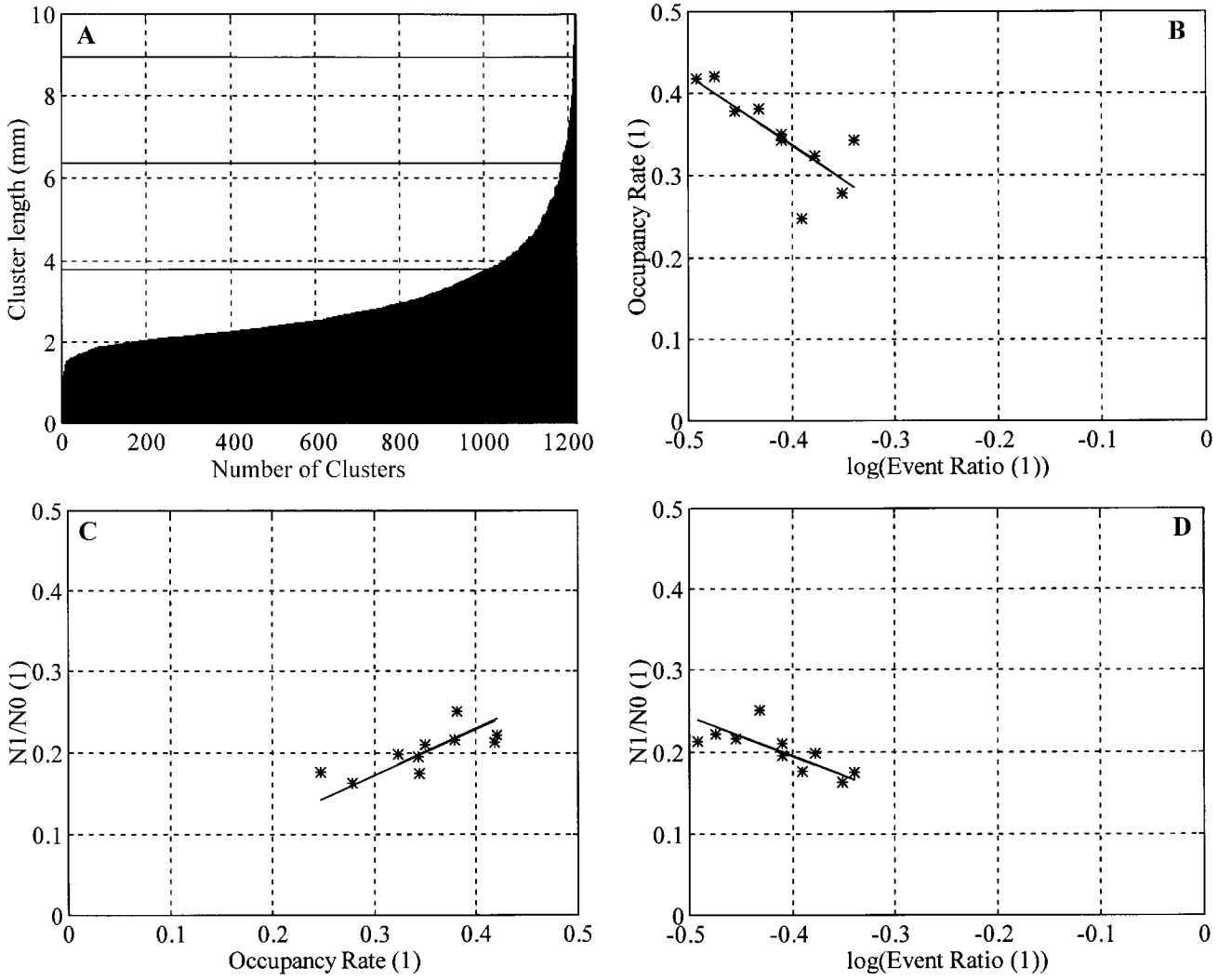

Figure 7. Measured sorted cluster lengths (*OR* = 0.42, 2000 initial particles) and functional relationships for urea fertilizer particles.

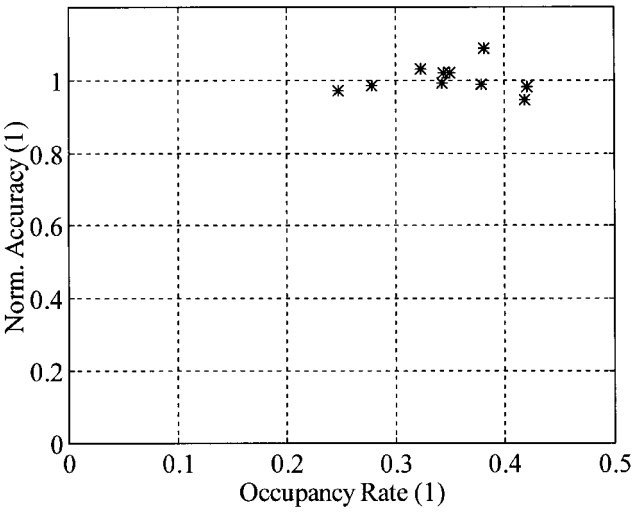

Figure 8. Normalized accuracy (1) of Exponential Estimator from 10 urea fertilizer experiments (2000 particles each).

Table 1. Exponential Estimator parameters for particles in simulation and experiment.

	$ER=e^{-\alpha_1 OR}$	$OR=\alpha_2 \frac{N_1}{N_0}$	$ER=e^{-\alpha_3 (N_1/N_0)}$
	α_1	α_2	α_3 (= $\alpha_1\alpha_2$)
Simulation			
Identical diameter	1	1	1
Urea fertilizer	1	1.8	1.8
Experiment			
Identical diameter	1.01	0.96	0.97
Urea fertilizer	1.19	1.74	2.07

The differences between simulation values and actual measurements found here do not imply that the measurement accuracy of the sensor is low. Rather, these differences imply that parameters α_1, α_2, and α_3 cannot be easily obtained by manually dropping particles through the sensor and then using the diameter distribution as simulation input to produce an accurate calibration factor. Instead, a test similar to the experiments described here needs to be carried out, and the α_3 value must be obtained from regression.

Conclusions

A device was developed that measures the mass flow of granular fertilizer in a high–density flow regime. By measuring the lengths of particle clusters and using a reconstruction algorithm based on simulation results, the mass flow of identical 4.45 mm particles was measured with an accuracy of 3% under high–density flow conditions. For granular fertilizer, the flow was measured with an accuracy of 2% for high–density/low–velocity flows, and 4% for high–velocity/low–density flows. All experiments were carried out under laboratory conditions.

The detection speed of the optical sensor was quite satisfactory. In some tests, over 550 clusters were detected per second, but the accuracy deteriorates for occupancy rates higher than 0.5. When the chosen time frame is longer, the accuracy can be expected to improve because more clusters would be involved in the measurements.

In practice, there would be a trade–off between rapidly updated mass flow indication and accuracy. The optical sensor should be placed in a location where the flow is high–velocity/low–density. The optimal location is at the rear of an aerial spreader, which is also advantageous when retrofitting existing equipment.

References

Bansal, R. K. 1997. Computer simulation of granular material flow in aerial spreaders. Ph.D. diss., University of Arkansas, Fayetteville, Ark.

Gardisser, D. R., and J. T. Walker. 1990. Adjustment of granular spreaders on agricultural aircraft. NAAA/ASAE Joint Technical Session. ASAE Paper AA90–003. St. Joseph, Mich.: ASAE.

Grift, T. E., and J. W. Hofstee. 1997. Measurement of velocity and diameter of individual fertilizer particles by an optical method. *J. Agric. Eng. Res.* 66(3): 235–238.

Grift, T. E., J. T. Walker, and D. R. Gardisser. 2000. Spread pattern analysis tool (SPAT): II. Examples of aircraft pattern analysis. *Trans. ASAE* 43(6): 1351–1362.

Grift, T. E. 2001. Mass flow measurement of granular materials in aerial application — Part 1: Simulation and modeling. *Trans. ASAE* 44(1): 19–22.

Helms, R. S., T. J. Siebenmorgen, and R. J. Norman. 1987. The influence of uneven preflood nitrogen distribution on grain yields of rice. *Arkansas Farm Research* (March–April). Fayetteville, Arkansas: University of Arkansas, Agricutural Experiment Station.

MatLab, ver. 5.0. 1997. Natick, Mass.: The Math Works, Inc.

Sall, J., and A. Lehman. 1996. *JMP Start Statistics*. Belmont, Calif.: Wadsworth Publishing Co.